Marine and Coastal Fisheries: Dynamics, Management, and Ecosystem Science 11:248–257, 2019

ISSN: 1942-5120 online
DOI: 10.1002/mcf2.10073

ARTICLE

Bottom Currents Affect Spanner Crab Catch Rates in Southern Queensland, Australia

David M. Spencer*
School of Engineering and Built Environment, Griffith University, Gold Coast, Queensland 4222, Australia; and SARDI Aquatic Sciences, Adelaide, South Australia 5024, Australia

Ian W. Brown
5 Baringa Street, Clontarf, Brisbane, Queensland 4019, Australia

Mark J. Doubell and Richard McGarvey
SARDI Aquatic Sciences, Adelaide, South Australia 5024, Australia

Shing Y. Lee
Simon F. S. Li Marine Science Laboratory, School of Life Sciences, and Earth System Science Programme, The Chinese University of Hong Kong, Sha Tin, New Territories, Hong Kong Special Administrative Region, China

Charles J. Lemckert
Built Environment and Design, University of Canberra, Canberra, Australian Capital Territory 2617, Australia

Abstract

During daily fishing operations, spanner crab *Ranina ranina* catch rates can fluctuate substantially, but the environmental drivers responsible for these fluctuations largely remain unresolved. Earlier research suggests that spanner crab catchability increases with strengthening currents, but uncertainties surround the magnitude of the measured current speeds and, consequently, their relationship with catch rates. Here, we explore the effects of bottom currents on spanner crab catch rates in South East Queensland, Australia. Using generalized additive mixed modeling, our results indicated that strengthening current speeds increased catch rates until reaching approximately 0.15 m/s, at which point the catch rates began to gradually decline. Results from a general linear regression model also showed that between fishing periods carried out on the same day, catch rates increased or decreased concurrently with current speeds. We conclude that bottom current speed should be considered in future stock assessment models. Better understanding the processes responsible for changes in bottom current speed will enable more accurate estimates of spanner crab population densities in the Australian fishery and will benefit the economic efficiency of commercial crabbing operations. Furthermore, future studies that investigate the effects of current speed on catch rates for other crab species should consider differences in locomotory characteristics and how they may impact the foraging efficiency of crabs under different flow conditions.

Subject editor: Anne B. Hollowed, Alaska Fisheries Science Center, Seattle

*Corresponding author: david.spencer2@griffithuni.edu.au
Received September 25, 2018; accepted March 20, 2019

Spanner crabs *Ranina ranina* are large marine brachyurans that inhabit coastal waters throughout the Indo-Pacific (Baylon and Tito 2012; Thomas et al. 2013). They are of significant economic importance in Australia, with gross landings contributing approximately AUD$5 million to the Queensland economy (Campbell et al. 2016). The Australian fishery operates with approximately 50 commercial vessels across the jurisdictional waters of Queensland and New South Wales, from approximately 22°S to 29°S (O'Neill et al. 2010; Campbell et al. 2016). Between December 20 and November 20 (note that from 2018, the fishery closure period changed to November 1–December 15), commercial spanner crab fishermen work under an individual transferable quota system and a total allowable commercial catch (Dichmont and Brown 2010) that is currently set at 947 metric tons (J. McGilvray, Department of Agriculture and Fisheries, Queensland, personal communication). Recent signs of a fishery-wide population decline have prompted an investigation into the possible reasons and the reliability of currently used indicators of spanner crab abundance. Developing a better understanding of the environmental causes of variation in the abundance and distribution of fishery stocks is key to successful management (Bacha et al. 2017; Spencer et al. 2017).

Population abundances of crab stocks can fluctuate greatly and may be related to environmental factors that occur at different temporal scales. For example, variations in the recruitment of red king crab *Paralithodes camtschaticus*, tanner crab *Chionoecetes bairdi*, blue king crab *Paralithodes platypus*, and snow crab *Chionoecetes opilio* have been linked to decadal climate shifts associated with changes in physical oceanographic processes (i.e., water column mixing) that affect the supply of food to crab larvae (Zheng and Kruse 2000, 2006). Decadal-scale changes in spanner crab stock density have also been linked to climate indices, as catch rates have been found to increase during El Niño years (Brown et al. 2008). Spanner crab catch rates also fluctuate seasonally, with higher CPUEs in spring and summer than in autumn and winter months. Skinner and Hill (1986, 1987) attributed this largely to the crabs' reproductive and molting cycles, but recent work has also linked seasonal upwelling to higher catch rates via a phenological response to foraging and searching for a mate (Spencer et al. 2019). Although earlier research found no significant difference in catch rates between morning and afternoon (Brown 1986), catch rates can vary substantially during daily fishing operations.

During daily crabbing operations, spanner crabs are caught in coastal waters generally at depths from 30 to 80 m by using flat tangle nets (~1 m^2 in area; Sumpton et al. 1995; Dichmont and Brown 2010). Typically baited with Australian Pilchards *Sardinops sagax neopilchardus*, the nets are spaced 50–60 m apart on groundlines and are soaked for periods ranging from 30 min to 2–3 h (Brown et al. 2008; Dichmont and Brown 2010). Once spanner crabs detect the bait odor, they emerge from the substrate and move considerable distances (up to ~70 m) upstream toward the baited nets (Skinner and Hill 1987; Hill and Wassenberg 1999). Successful fishing therefore depends on bottom currents to facilitate the dispersal of the bait odor plume (e.g., Finelli 2000; Westerberg and Westerberg 2011; Taylor et al. 2013) to populations of spanner crabs downstream.

In a study of the spanner crab fishery in northern New South Wales, Craig and Kennelly (1991) found a positive linear relationship between bottom current speed and catch rates, suggesting that the effective fishing area of the traps is proportional to the local current speeds. In contrast, the foraging efficiency of blue crabs *Callinectes sapidus* and green crabs *Carcinus maenas* was found to decrease in stronger currents of approximately 0.14 and 0.23–0.58 m/s, respectively (Weissburg and Zimmer-Faust 1993; Weissburg et al. 2003; Robinson et al. 2011). Current speeds measured by Craig and Kennelly (1991) were in excess of 1.5 m/s, with maximum speeds reaching 6 m/s, which are unusually strong for this area. More recent studies have shown that similar shelf habitats in South East Queensland are typically characterized by bottom and near-bottom (~3 m above the seabed) current speeds of 0.03–0.15 m/s (Hill and Wassenberg 1999) and 0.1–0.27 m/s (Spencer et al. 2017), respectively—less than 5% of the maxima reported earlier by Craig and Kennelly (1991). Consequently, the effect of current speed on spanner crab catch rates deserves further attention, as there may be a point at which strengthening currents begin to reduce the ability of the crabs to forage effectively, leading to a change in their catchability.

In this paper, we investigate the effects of bottom current speed and direction and tidal phase on spanner crab catch rates and explore whether changes in current patterns during daily fishing operations are responsible for short-term (same-day) variation in CPUE.

METHODS

Study region.— Crab catch, effort, and hydrodynamic data were collected from a 10-m commercial spanner crab vessel operating off the Gold Coast, Queensland, Australia. Fishing locations, chosen by the vessel's skipper, ranged from South Stradbroke Island south to the Queensland–New South Wales border (Figure 1). Fishing took place in two distinct areas (A_1 and A_2) approximately 12–20 km offshore at depths between 50 and 80 m (Figure 1). Within this area, the shelf seafloor consists mainly of sandy sediment (medium-fine grain size) with patches of hard substrate, including rocky reefs (Marshall

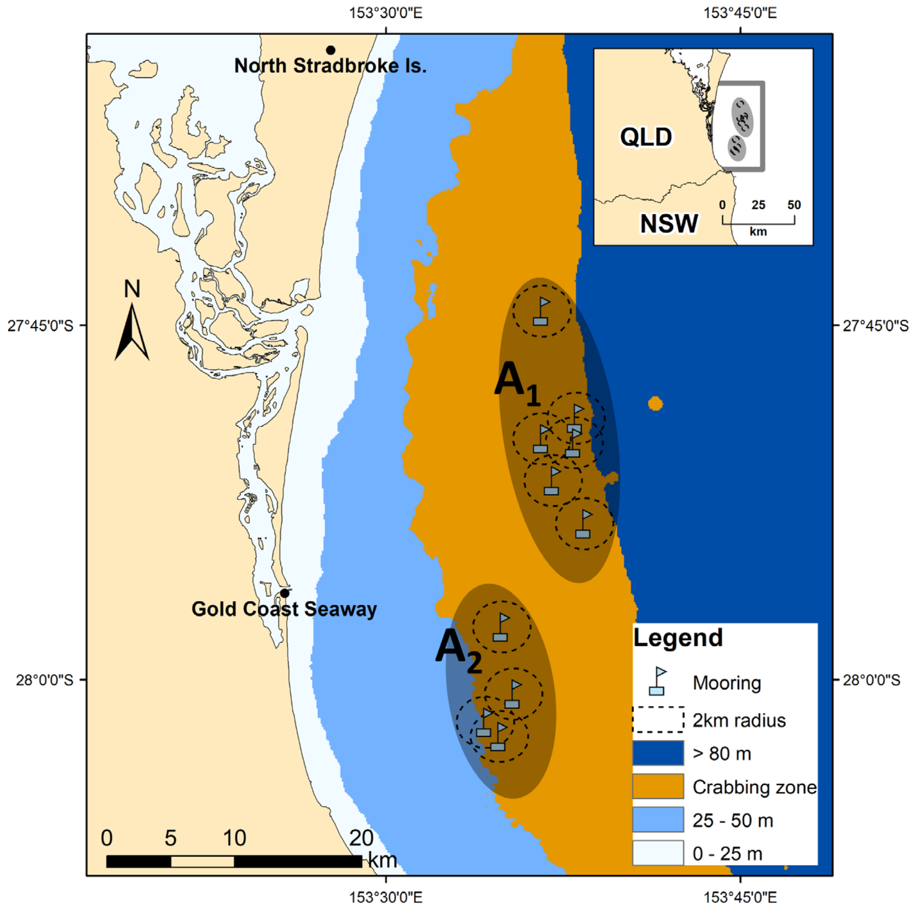

FIGURE 1. Fishing for spanner crabs was carried out in two distinct areas (area 1 [A_1] and area 2 [A_2]) off the Gold Coast, Australia (QLD = Queensland; NSW = New South Wales). Locations of the oceanographic mooring (flag symbols) and corresponding daily fishing locations (dotted circles) are shown for the study period (June 2015–September 2016). The orange area encloses the 50–80-m depth range, where spanner crabbing is typically carried out in this region.

and Oldham 1980; Richmond and Stevens 2014). Fishing was conducted at least 1–2 km from reef areas to avoid snagging the fishing gear and because spanner crabs are typically found on flat, sandy substrates (Brown et al. 2008).

Mooring materials and design.— A lightweight, compact mooring was designed for short-term deployment and recovery from the crabbing vessel. A polyform teardrop "A-Series" buoy with an attached pole-mounted flag was used as the surface marker. This was attached by a length of 12-mm polypropylene mooring line, approximately 1.5 times the depth of the water, to a marine-grade, stainless-steel frame with a 20-kg weight bolted to its base. Hydrodynamic data were collected using a Nortek Vector acoustic Doppler velocimeter (ADV) and a Nortek Aquadopp acoustic Doppler current profiler (ADCP) attached near the base of the mooring line. The upward-facing ADCP was attached to the mooring line about 1.5 m above the seafloor and suspended in the water column from a 0.3-m polystyrene float placed 10 m above the sensor head. The ADV was placed inside the steel frame anchored to the seabed, with the flexible sensor head facing upward and fixed above the frame (~0.5 m above the seabed) to collect unobstructed, near-bottom current velocity data.

Crab catch and effort data.— Field studies were carried out opportunistically when the fishing days, locations, and times chosen by the vessel's skipper were appropriate. Catch and effort data were derived from 10 fishing days during the periods June–October 2015 and August–September 2016. On arrival at the chosen fishing site, the instrument mooring was deployed, and fishing operations were conducted within a 2-km radius of the mooring. Spanner crabs were caught by using industry standard tangle nets comprising a single layer of ~50-mm-mesh net made of 2-mm-diameter monofilament nylon tightly strung across flat rectangular frames (e.g., Hill and Wassenberg 1999). Clipped to the center of each net were bait holders filled with Australian Pilchards before each deployment. Due to the small aperture of the net mesh, the crabs' limbs become entangled as they move toward the bait. Fifteen nets, spaced approximately 60 m apart, were attached to each of three groundlines and were deployed on the seafloor across the shelf in an east–west direction. After 2–3 h, the first groundline was winched back onboard, legal-sized crabs were retained, and undersized crabs (rostral carapace length < 10 cm) were immediately discarded. The groundline was then redeployed at a second location within 2 km of the mooring. This process was repeated until all groundlines had been retrieved and reset. The fishing period is defined as the time elapsed between setting the first of the groundlines and retrieving the last of the groundlines.

Catch per unit effort was calculated as the total retained weight of legal-sized crabs divided by the total number of net-hours:

$$\mathrm{CPUE} = \frac{\text{total retained weight}}{\text{total net} - \text{hours}}, \tag{1}$$

where total retained weight was estimated from the number of bins filled (or partly filled) after each fishing period (one full bin contains ~22 kg of crab), and total net-hours were the product of the total number of net lifts and the sum of soak times (h) in each fishing period (Brown et al. 2008).

Hydrodynamic data.— The ADV and ADCP instruments each collected 1-Hz current velocity data, sampling 1-min averages at 5-min intervals. Raw data reported on the Cartesian coordinate system (XYZ) were cleaned by removing observations with a signal-to-noise ratio less than 5 dB or signal correlation values less than 60% (Chanson et al. 2008). Cleaned ADCP data were then converted to Earth referenced units (east, north, up [ENU]) using Nortek Storm software (www.nortek.no). The ADCP measured current velocity in 5-m bins of the 40-m water column above the sensor head.

From the ADV data, single-point horizontal speed (m/s) was derived near the seabed as follows:

$$\text{Current speed} = \sqrt{x^2 + y^2}, \tag{2}$$

where x and y are the east–west and north–south components, respectively. Current direction was then calculated using

$$\text{Current direction} = \mathrm{MOD}[\arctan 2(x, y) \times 180/\pi, 360°]. \tag{3}$$

The modulo (MOD) inverse tangent was used to avoid negative degrees and correct for true current direction (www.nortek.no). For simplicity, direction of travel was split into four components: north (316–45°), east (46–135°), south (136–235°), and west (236–315°). The ADV's pressure sensor provided depth data, allowing changes in tidal phase to be monitored throughout the observation period.

Statistical analyses.— Spatiotemporal and hydrodynamic effects on CPUE were analyzed using generalized additive mixed models (GAMMs) with the package "mgcv" (Wood 2012). A thin plate regression spline with a predefined number of knots ($k = 3$) was used to avoid overfitting when analyzing the effects of mean current speed on catch rates (Wood 2003, 2017; Zuur et al. 2009; Marra and Wood 2011). Seasonal effects on catch rates (e.g., Brown 1986; Skinner and Hill 1986, 1987; Spencer et al. 2019) were modeled by treating month as a continuous variable, which was also smoothed using thin plate regression and restricted to three knots to avoid overfitting between only two seasons (winter and spring). Tidal phase (ebb, flood, or slack tide) and current direction (north, south, east, or west) were modeled as discrete (categorical) terms (Zuur et al. 2009). Fishing area (A_1 and A_2; Figure 1) and year were also included in the models as discrete terms to account for spatial and temporal changes in abundance, respectively. To account for similarities in near-bottom hydrodynamics on a given fishing day, "day" was included as a discrete random effect (Wood 2012).

The GAMM assumptions were met (see diagnostics in the Supplementary Material available separately online) by normalizing CPUE using a natural logarithm transformation and modeling the transformed CPUE with Gaussian errors (Brown et al. 2008; Zuur et al. 2009). The initial GAMM was set up using all explanatory variables and then optimized by stepwise elimination of the least significant variable (highest $P > 0.05$; Feekings et al. 2015). For the final model, an a priori model selection method was used for multiple GAMMs that shared similar corrected Akaike's information criterion (AIC_c) and Bayesian information criterion (BIC) scores (Hurvich and Tsai 1989; Burnham and Anderson 2004; Barton 2009). This ensured that all informative explanatory variables were retained in the final model (Arnold 2010).

Changes in CPUE and mean current speed and direction were determined by calculating the difference between two fishing periods within the same day. Days in which there were two fishing periods resulted in only one change (i.e., period 2 minus period 1), while those with three fishing periods resulted in three changes throughout the day (i.e., period 2 minus period 1; period 3 minus period 2; and period 3 minus period 1). Across all 10 fishing days, general linear regression models were used to analyze the effects of changes in current speed and direction on changes in CPUE. Positive or negative values represent an increase or decrease (respectively) in CPUE and current speed. Change in current direction ranged from 0° to 180°, with 0° being no change and 180° being a complete reversal in current direction. All statistical analyses were carried out in the R statistical environment (R Development Core Team 2018).

RESULTS

Twenty-six fishing periods were recorded over the 10 fishing days between June 2015 and September 2016 (Table 1). Three fishing periods were carried out on 6 of the 10 fishing days, and two fishing periods were carried out on the other 4 d, resulting in a total of 22 changes in CPUE and near-bottom current speed and direction. After each fishing period, CPUE ranged from 0.13 to 1.83 kg/net-hour. During each fishing period, mean near-bottom current speed measured by the ADV ranged from 0.03 to 0.21 m/s. Tidal phase varied between ebb, flood, and slack tide for each fishing period, and the mean current direction was prevalently traveling offshore (east), with only a small number of periods when the predominant direction was north, south, or west.

From the initial GAMM, stepwise elimination of the least significant variable (highest $P > 0.05$) resulted in removal of year, tidal phase, fishing area, and current direction. The model of best fit (with the lowest AIC_c and BIC scores) contained current speed and day (Table 2). However, four models containing various combinations of day, month, and current speed yielded similar AIC_c, BIC, and log-likelihood values, indicating that each of the explanatory variables was informative and that the model (final model) best suited to our data incorporated all three variables (Table 2). In the final model, the estimated effects of current speed on catch rates showed that when CPUE was low, mean current speeds were also low (Figure 2; negative linear predictor values). As current speed increased, catch rates increased until reaching approximately 0.15 m/s (positive linear predictor values), beyond which they trended slightly downward but with a much higher degree of uncertainty. Month had a significant effect ($P < 0.05$) on

TABLE 1. Spanner crab CPUE and hydrodynamic data for all fishing periods carried out in each area (A_1 and A_2; see Figure 1) over the 10 fishing days. Fishing period constitutes the time elapsed between deployment of the first groundline and retrieval of the last groundline (not counting the same groundline more than once). Tidal phase was determined by the most pronounced stage of the tidal cycle during each fishing period.

Fishing day	Fishing period (hours)	Area	Current speed (m/s)	Current direction (degrees)	Tidal phase	CPUE (kg/net-hour)
Day 1	0625–0845	A_1	0.11	215	Slack	0.54
	0830–1035		0.08	225	Ebb	0.27
Day 2	0700–0920	A_1	0.17	120	Flood	0.28
	0905–1130		0.21	120	Flood	0.49
	1115–1330		0.21	110	Flood	0.36
Day 3	0745–0945	A_1	0.07	220	Slack	0.18
	0800–1100		0.06	245	Ebb	0.13
	1115–1445		0.08	170	Ebb	0.72
Day 4	0600–0805	A_2	0.15	55	Ebb	0.88
	0750–1020		0.15	55	Slack	0.7
	1000–1150		0.14	60	Flood	1.02
Day 5	0645–0900	A_2	0.14	50	Flood	0.96
	0845–1050		0.13	60	Ebb	0.56
Day 6	0640–0900	A_2	0.07	50	Flood	1.29
	0930–1130		0.08	60	Ebb	1.83
Day 7	0645–0900	A_1	0.04	280	Slack	0.43
	0850–1100		0.09	250	Flood	0.76
	1045–1355		0.10	275	Flood	0.75
Day 8	0545–0830	A_1	0.09	95	Ebb	0.8
	0815–1130		0.09	105	Ebb	0.83
Day 9	0615–0845	A_1	0.11	315	Ebb	0.59
	0830–1130		0.09	320	Ebb	0.57
	1100–1230		0.10	310	Flood	0.98
Day 10	0530–0800	A_2	0.04	235	Flood	0.2
	0745–1100		0.04	115	Flood	0.26
	1045–1330		0.06	85	Ebb	0.49

catch rates, with CPUE increasing linearly from June to October (winter to spring; Figure 2).

Changes in CPUE between fishing periods on the same day ranged from about 0 to 0.6 kg/net-hour. Changes in mean current speed and direction ranged from 0 to 0.06 m/s and from 0° to 150°, respectively. The general linear regression model indicated that the effect of current direction on CPUE was weak ($P > 0.05$, $r^2 = 0.05$), but there was a stronger, positive correlation between mean current speed and catch rates ($P < 0.05$; Figure 3). An atypical increase in CPUE (~400%) from fishing periods 1 and 2 to fishing period 3 on day 3 (August 2015) may have been due to the stronger current traveling 30 m above the seafloor that migrated into the bottom boundary layer, as indicated by the ADCP data in Figure 4.

TABLE 2. Comparison between the top-four generalized additive mixed models after stepwise elimination of independent variables with the highest P-value (when $P > 0.05$). The final model (in bold) was chosen based on the top-three models sharing similar corrected Akaike's information criterion (AIC_c), Bayesian information criterion (BIC), and log-likelihood (Log$L$) scores, indicating that all three explanatory variables are informative (s = thin plate regression spline; k = number of knots).

Model	AIC_c	BIC	Log$L$
s(current speed, k = 3), random = list(day = ~1)	51.9	55.2	−19.4
s(month, k = 3) + s(current speed, k = 3)	52.7	55.8	−18.1
s(month, k = 3), random = list(day = ~1)	52.7	56	−19.9
s(current speed, k = 3) + s(month, k = 3), random = list(day = ~1)	**54.2**	**56.8**	**−17**

DISCUSSION

The range of current speeds we observed agreed well with measurements by Hill and Wassenberg (1999) in the South East Queensland region but was one to two orders of magnitude lower than values reported by Craig and Kennelly (1991) on the mid-coast of New South Wales, some 50 km south of our study area. This disparity may be due to the characteristics of the current meter used in the earlier study, which means that the relationship between current speed and catch rates described by Craig and Kennelly (1991) remains open to question (Spencer et al. 2017).

Our results show a nonlinear relationship between mean bottom current speed and spanner crab catch rates, with CPUEs increasing with current speed until peaking at approximately 0.15 m/s (~0.3 knots). Beyond this point, catch rates began to decline, but the associated effects were highly ambiguous, which is likely due to the limited number of fishing periods in which current speeds exceeded 0.15 m/s. Year and fishing area were eliminated from the model, indicating that there was no significant difference in adjusted spanner crab population density between 2015 and 2016 and between A_1 and A_2, respectively. Seasonal and day-to-day variations in catch rates were important and impacted the effect of current speed ($P = 0.06$) in the final model. The general linear regression model, which accounted for seasonal and random daily effects, showed a positive correlation between changes in catch rates and changes in current speed

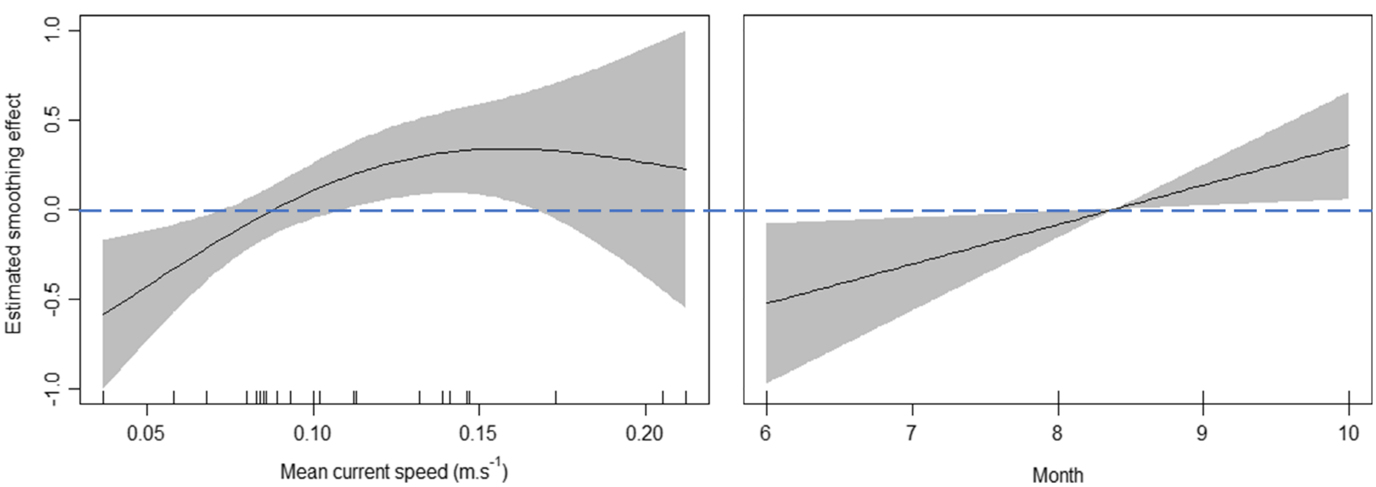

FIGURE 2. The effects of mean current speed (m/s) and month on spanner crab catch rates across all fishing days. Results are reported on the scale of the linear predictor (y-axis). The curved line indicates the fit of the regression spline (centered for model identifiability), and shaded areas are the 95% confidence bands of the model. The rug plots on the x-axes show the values of the explanatory (independent) variables.

between fishing periods on the same day. Overall, both analyses indicated a positive relationship between catch rates and current speeds ranging from 0.04 to 0.15 m/s, but beyond this point, catch rates may start to decline, probably due to impairment of the crabs' foraging efficiency.

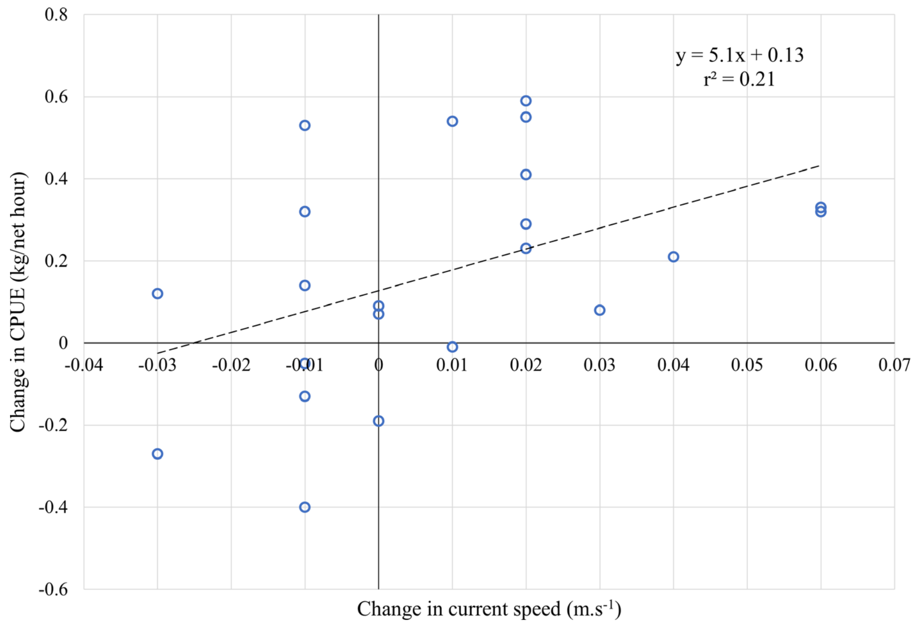

FIGURE 3. The effect of changes in current speed (m/s) on changes in spanner crab CPUE (kg/net-hour) between two fishing periods carried out on the same day. Positive and negative values on both axes correspond with increases and decreases, respectively, in current speed or catch rate.

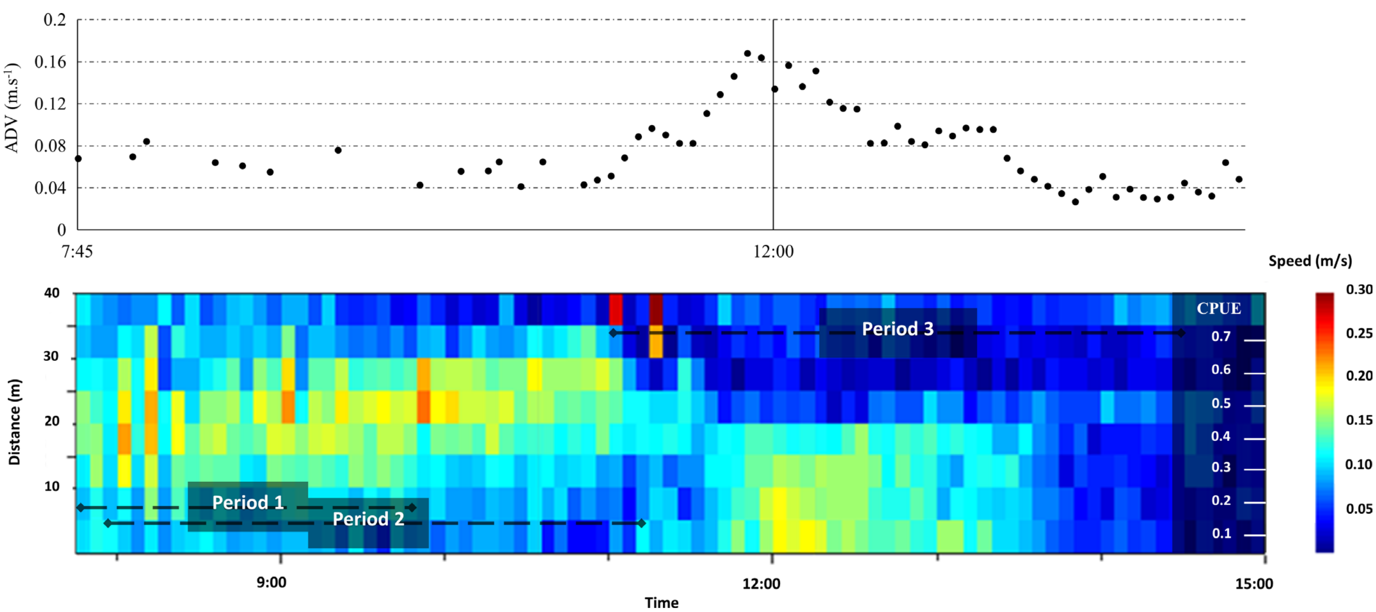

FIGURE 4. Time series of acoustic Doppler velocimeter (ADV; top) and acoustic Doppler current profiler (ADCP; bottom) data on day 3 (see Table 1). Gaps in the ADV time series are the result of removing erroneous data. The ADCP profile is shown as a function of current speed above the sensor head (~2.5 m above the seabed). The placement of "Period (1, 2, or 3)" denotes the mean CPUE (kg/net-hour; secondary *y*-axis) and soak time (length of the line relative to the *x*-axis) from each fishing period. Each row of rectangles represents the current speed (m/s) averaged over 5-m bins of the 40-m profile every 5 min.

In the Damariscotta River, Maine, Robinson et al. (2011) reported higher catch rates of green crabs at sites with weak currents (0.05–0.11 m/s) than at sites with strong currents (0.23–0.58 m/s). Those results are not directly comparable to ours because we did not record persistent current flows within the range of their "strong" currents, which is likely due to differences in habitat hydrodynamics (i.e., riverine versus shelf waters). There is, however, a clear distinction between spanner crabs' and blue crabs' ability to forage in a similar range of current speeds (0.03–0.14 m/s; Weissburg and Zimmer-Faust 1993). This distinction may be related to differences in the species' locomotory behavior when scavenging for food. Weissburg et al. (2003) reported that blue crabs orientate themselves at an angle (0–90°) relative to the flow direction that is optimized by minimizing the drag forces imposed on their bodies when facing into the current and maximizing their ability to detect odor plumes. Drag forces increase when current speeds are stronger (0.14 m/s); thus, blue crabs were found to sacrifice their ability to detect bait, resulting in a reduction in foraging efficiency (Weissburg et al. 2003). Unlike blue crabs and other crab species, which move in a sideways motion, spanner crabs move forward upstream by "punting" and swimming toward the food source (Faulkes 2006). As a result, spanner crabs do not need to orientate their bodies at an angle relative to the flow direction, and their ability to detect bait plumes would be unaffected by the cost of locomotion that blue crabs endure.

The observed range of current speeds in our study has also been described elsewhere as creating different plume structures along sandy substrates (Weissburg and Zimmer-Faust 1993; Zimmer-Faust et al. 1995), which can affect the area and/or concentration of the bait odor. Over a short distance of about 3 m, Zimmer-Faust et al. (1995) found that weak (0.04 m/s), intermediate (0.1 m/s), and strong (0.25 m/s) currents generated plumes with different horizontal advective and dispersion properties. Intermediate current speeds appeared to optimize the advection and dispersion properties of the bait plume in the immediate surroundings and at the furthest distance from the source of the odor. Plumes generated by intermediate current speeds (~0.14 m/s) were also more restricted vertically, remaining closer to the seafloor (Weissburg and Zimmer-Faust 1993). This would presumably reduce the loss of bait odor into the water column beyond the spanner crabs' demersal habitat (Kirkwood et al. 2005; Faulkes 2006) and would benefit the attraction of spanner crabs at much greater distances downstream (e.g., up to 70 m; Hill and Wassenberg 1999).

Recommendations for Future Work

For financial reasons, the experimental design of our work was limited to 10 fishing days randomly distributed across 2 years (and only two seasons) as a result of relying on a commercial spanner crab vessel and the availability of oceanographic equipment. Our data did not reveal notable differences in current speeds between months (e.g., Spencer et al. 2017), but future work should investigate the effect of current speed on catch rates at other times of the year, as Skinner and Hill (1987) found that spanner crabs spend a considerable amount of time inactive during the post-molt period in austral autumn months. Although few undersized crabs were caught during our study, discards should be accounted for in future studies if the proportion of sublegal crabs in the catch is substantial. Further investigations using underwater video apparatus attached to baited tangle nets (e.g., Brown 2012), in conjunction with hydrodynamic data, would also allow oceanographic influences occurring over short periods to be more precisely related to spanner crab activity.

Conclusion

This work has helped to elucidate the uncertainties surrounding the effects of current speed on spanner crab catch rates. Using moored oceanographic instruments, we were able to relate catch rates to accurate measures of current speed, thereby highlighting the importance of using reliable oceanographic instruments. We also showed that over a range of current speeds from 0.04 to 0.15 m/s, the catch rates of spanner crabs were higher when currents were stronger. The difference in the effect of current speed on the foraging abilities of spanner crabs and blue crabs was attributed to differences in their locomotory characteristics. This particular finding has global implications for future studies investigating the effects of current speed on catch rates of other exploited demersal crustacean species.

A calibrated operational hydrodynamic model that is capable of resolving bottom boundary layer dynamics across the spanner crab fishery would greatly benefit this work. Specifically, a hydrodynamic model that can reproduce and forecast reliable bottom current speed data could help to improve spanner crab catch standardization and stock assessment models. It would also help to identify reasons for inexplicable anomalies in apparent spanner crab population densities—a recurring issue with stock assessment model outputs. Better understanding the processes responsible for changes in current speed would also benefit these models and would allow commercial fishermen to use the information for strategic fishing to improve the economic efficiency of the industry.

ACKNOWLEDGMENTS

D.M.S. dedicates this work to commercial fishermen Richard Hamilton and Mark Cheeseman for their invaluable assistance with data collection and mooring deployments, including fishing days that involved “trial and error” during the design stages of the mooring. This project was also supported by the Griffith School of Engineering and Built Environment, including staff Chuen Lo and Geoff Turner, who provided helpful advice with respect to mooring design and the various materials used. There is no conflict of interest declared in this article.

REFERENCES

Arnold, T. W. 2010. Uninformative parameters and model selection using Akaike's information criterion. Journal of Wildlife Management 74:1175–1178.

Bacha, M., M. A. Jeyid, V. Vantrepotte, D. Dessailly, and R. Amara. 2017. Environmental effects on the spatio-temporal patterns of abundance and distribution of *Sardina pilchardus* and sardinella off the Mauritanian coast (north-west Africa). Fisheries Oceanography 26:282–298.

Barton, K. 2009. MuMIn: multi-model inference. R package version 0.12.0.

Baylon, J. C., and O. D. Tito. 2012. Natural diet and feeding habits of the red frog crab (*Ranina ranina*) from southwestern Mindanao. Philippines. Philippine Agricultural Scientist 95:391–398.

Brown, I. W. 1986. Population biology of the spanner crab in South-East Queensland. Southern Fisheries Centre, Department of Primary Industries, Final Project Report, Brisbane, Queensland, Australia.

Brown, I. W. 2012. Assessing the value of spatial closures to exploited demersal crustacean communities in the Moreton Bay Marine Park. Department of Environment and Resource Management and Agri-Science, Final Project Report, Brisbane, Queensland, Australia.

Brown, I. W., J. Scandol, D. Mayer, M. Campbell, S. Kondylas, M. McLennan, A. Williams, K. Krusic-Golub, and T. Treloar. 2008. Reducing uncertainty in the assessment of the Australian spanner crab fishery. Department of Primary Industries and Fisheries, Project Report PR07-3314, Brisbane, Queensland, Australia.

Burnham, K. P., and D. R. Anderson. 2004. Multimodel inference: understanding AIC and BIC in model selection. Sociological Methods and Research 33:261–304.

Campbell, M., M. O'Neill, and J. McGilvray. 2016. Queensland spanner crab fishery: commercial quota setting for June 2015–May 2016. Report to the Queensland Department of Agriculture and Fisheries, Brisbane, Queensland, Australia.

Chanson, H., M. Takeuchi, and M. Trevethan. 2008. Using turbidity and acoustic backscatter intensity as surrogate measures of suspended sediment concentration in a small subtropical estuary. Journal of Environmental Management 88:1406–1416.

Craig, J., and S. Kennelly. 1991. An inexpensive instrument for measuring benthic current velocity and direction at sea. Estuarine, Coastal, and Shelf Science 32:633–638.

Dichmont, C. M., and I. W. Brown. 2010. A case study in successful management of a data-poor fishery using simple decision rules: the Queensland spanner crab fishery. Marine and Coastal Fisheries: Dynamics, Management, and Ecosystem Science [online serial] 2:1–13.

Faulkes, Z. 2006. The locomotor toolbox of the spanner crab, *Ranina ranina* (Brachyura, Raninidae). Crustaceana 79:143–155.

Feekings, J., A. Christensen, P. Jonsson, R. Frandsen, M. Ulmestrand, S. Munch-Petersen, and B. Andersen. 2015. The use of at-sea-sampling data to dissociate environmental variability in Norway lobster (*Nephrops norvegicus*) catches to improve resource exploitation efficiency within the Skagerrak/Kattegat trawl fishery. Fisheries Oceanography 24:383–392.

Finelli, C. M. 2000. Velocity and concentration distributions in turbulent odor plumes in the presence of vegetation mimics: a flume study. Marine Ecology Progress Series 207:297–309.

Hill, B. J., and T. J. Wassenberg. 1999. The response of spanner crabs (*Ranina ranina*) to tangle nets—behaviour of the crabs on the nets, probability of capture and estimated distance of attraction to bait. Fisheries Research 41:37–46.

Hurvich, C. M., and C. Tsai. 1989. Regression and time series model selection in small samples. Biometrika 76:297–307.

Kirkwood, J., I. Brown, S. Gaddes, and S. Hoyle. 2005. Juvenile length-at-age data reveal that spanner crabs (*Ranina ranina*) grow slowly. Marine Biology 147:331–339.

Marra, G., and S. N. Wood. 2011. Practical variable selection for generalized additive models. Computational Statistics and Data Analysis 55:2372–2387.

Marshall, J. F., and W. Oldham. 1980. Continental shelf sediments: southern Queensland and northern New South Wales. Bureau of Mineral Resources, Geology, and Geophysics, Bulletin 207, Canberra, Australia.

O'Neill, M. F., A. B. Campbell, I. W. Brown, and R. Johnstone. 2010. Using catch rate data for simple cost-effective quota setting in the Australian spanner crab (*Ranina ranina*) fishery. ICES Journal of Marine Science 67:1538–1552.

R Development Core Team. 2018. R: a language and environment for statistical computing. R Foundation for Statistical Computing, Vienna.

Richmond, S., and T. Stevens. 2014. Classifying benthic biotopes on subtropical continental shelf reefs: how useful are abiotic surrogates? Estuarine, Coastal, and Shelf Science 138:79–89.

Robinson, E. M., D. L. Smee, and G. C. Trussell. 2011. Green crab (*Carcinus maenas*) foraging efficiency reduced by fast flows. PLoS One [online serial] 6(6):e21025.

Skinner, D., and B. Hill. 1986. Catch rate and emergence of male and female spanner crabs (*Ranina ranina*) in Australia. Marine Biology 91:461–465.

Skinner, D., and B. Hill. 1987. Feeding and reproductive behaviour and their effect on catchability of the spanner crab *Ranina ranina*. Marine Biology 94:211–218.

Spencer, D. M., I. W. Brown, M. J. Doubell, C. J. Brown, A. Redondo Rodriguez, S. Y. Lee, H. Zhang, and C. J. Lemckert. 2019. Bottom boundary layer cooling and wind-driven upwelling enhance the catchability of spanner crab (*Ranina ranina*) in South-East Queensland, Australia. Fisheries Oceanography 28:317–326.

Spencer, D. M., I. W. Brown, S. Y. Lee, and C. J. Lemckert. 2017. Physical oceanographic processes affecting catchability of spanner crab (*Ranina ranina*)—a review. Fisheries Research 186:248–257.

Sumpton, W., I. Brown, and S. Kennelly. 1995. Fishing gears that minimise the damage incurred by discarded spanner crabs (*Ranina ranina*): laboratory and field experiments. Fisheries Research 22:11–27.

Taylor, M. D., J. Baker, and I. M. Suthers. 2013. Tidal currents, sampling effort and baited remote underwater video (BRUV) surveys: are we drawing the right conclusions? Fisheries Research 140:96–104.

Thomas, L. R., G. T. DiNardo, H.-H. Lee, K. R. Piner, and S. E. Kahng. 2013. Factors influencing the distribution of Kona crabs *Ranina ranina* (Brachyura: Raninidae) catch rates in the main Hawaiian Islands. Journal of Crustacean Biology 33:633–640.

Weissburg, M., C. James, D. Smee, and D. Webster. 2003. Fluid mechanics produces conflicting constraints during olfactory navigation of blue crabs, *Callinectes sapidus*. Journal of Experimental Biology 206:171–180.

Weissburg, M. J., and R. K. Zimmer-Faust. 1993. Life and death in moving fluids: hydrodynamic effects on chemosensory-mediated predation. Ecology 74:1428–1443.

Westerberg, H., and K. Westerberg. 2011. Properties of odour plumes from natural baits. Fisheries Research 110:459–464.

Wood, S. N. 2003. Thin plate regression splines. Journal of the Royal Statistical Society Series B: Statistical Methodology 65:95–114.

Wood, S. 2012. Package "mgcv": mixed GAM computation vehicle. R package version 1.8-23. Available: https://CRAN.R-project.org/package=mgcv. (April 2019).

Wood, S. N. 2017. Generalized additive models: an introduction with R. Chapman and Hall/CRC Press, Boca Raton, Florida.

Zheng, J., and G. H. Kruse. 2000. Recruitment patterns of Alaskan crabs in relation to decadal shifts in climate and physical oceanography. ICES Journal of Marine Science 57:438–451.

Zheng, J., and G. H. Kruse. 2006. Recruitment variation of eastern Bering Sea crabs: climate-forcing or top-down effects? Progress in Oceanography 68:184–204.

Zimmer-Faust, R. K., C. M. Finelli, N. D. Pentcheff, and D. S. Wethey. 1995. Odor plumes and animal navigation in turbulent water flow: a field study. Biological Bulletin 188:111–116.

Zuur, A. F., E. N. Ieno, N. J. Walker, A. A. Saveliev, and G. M. Smith. 2009. Mixed effects models and extensions in ecology with R. Springer-Verlag, New York.

SUPPORTING INFORMATION

Additional supplemental material may be found online in the Supporting Information section at the end of the article.